Supplementary Information (SI) for Dalton Transactions.
This journal is © The Royal Society of Chemistry 2024

Supporting information

Visible light-induced CO releasing properties and cytotoxicity of Ru(II) carbonyl complex with 2-(pyridin-2-yl)-quinoxaline

Rabaa M. Khaled, [a1] Mahmoud T. Abo-Elfadl,[b,c1] Krzysztof Radacki, [d] Mona A. M. Abo-Zeid, [b, e] Nora S. Abdel-Kader, [a] Ola R. Shehab, [a] Gamal A. E. Mostafa, [f] Essam A. Ali, [f] Shaikha S. Al Neyadi, [g] and Ahmed M. Mansour,*[a,g1]

[a.] *Department of Chemistry, Faculty of Science, Cairo University, Gamma Street, Giza, Cairo 12613, Egypt.*

[b.] *Cancer Biology and Genetics Laboratory, Centre of Excellence for Advanced Sciences, National Research Centre, Dokki, Cairo 12622, Egypt*

[c.] *Biochemistry Department, Biotechnology Research Institute, National Research Centre, Dokki, Cairo 12622, Egypt.*

[d.] *Institut für Anorganische Chemie, Julius-Maximilians-Universität Würzburg, Am Hubland, D-97074 Würzburg, Germany.*

[e.] *Genetics and Cytology Department, Genetic Engineering and Biotechnology Research Institute, National Research Centre, Giza, Egypt.*

[f.] *Department of Pharmaceutical Chemistry, College of Pharmacy, King Saud University, Riyadh 11451, Saudi Arabia.*

[g.] *Department of Chemistry, United Arab Emirates University, Al-Ain, United Arab Emirates.*
Mansour_am@uaeu.ac.ae; mansour@sci.cu.edu.eg.; inorganic_am@yahoo.com

[1] *equal contribution.*

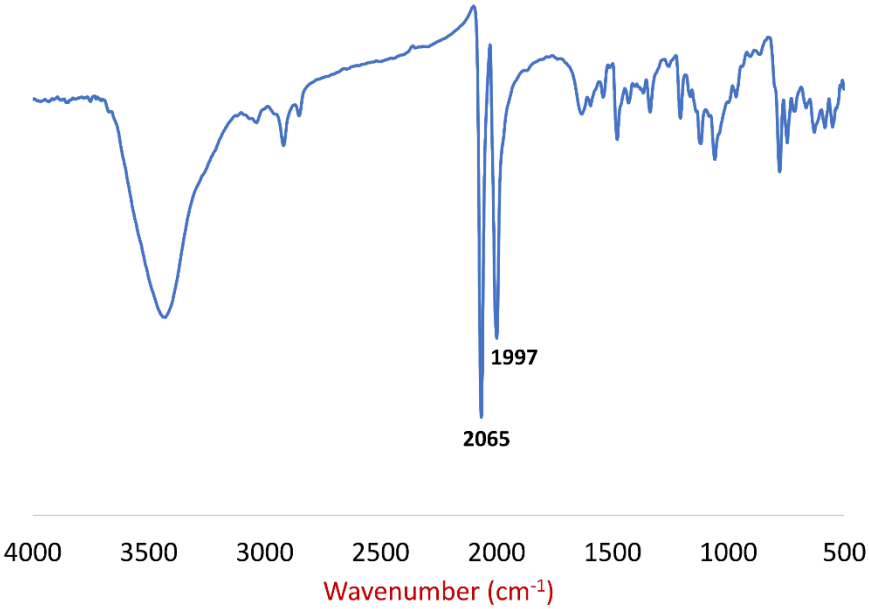

Fig. S1 IR spectrum of **2**.

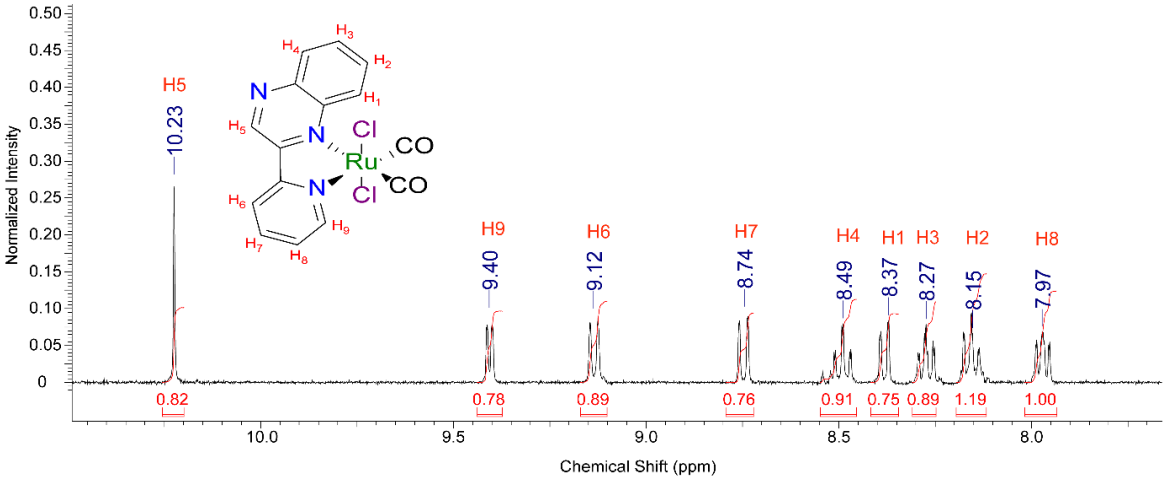

Fig. S2 ^{1}H NMR spectrum of **2** in DMSO-d_6 (Proton assignments (H1–H9) labelled according to the molecular structure).

Hydrogen Position	Approximate Chemical Shift (ppm)	Splitting Pattern	Coupling Constant (J in Hz)
H1	8.37	Doublet	8
H2	8.14	Triplet	16
H3	8.25	Triplet	12
H4	8.47	Doublet	8
H5	10.23	singlet	-
H6	9.12	Doublet	8
H7	8.74	Triplet	16
H8	7.95	Triplet	16
H9	9.40	Doublet	8

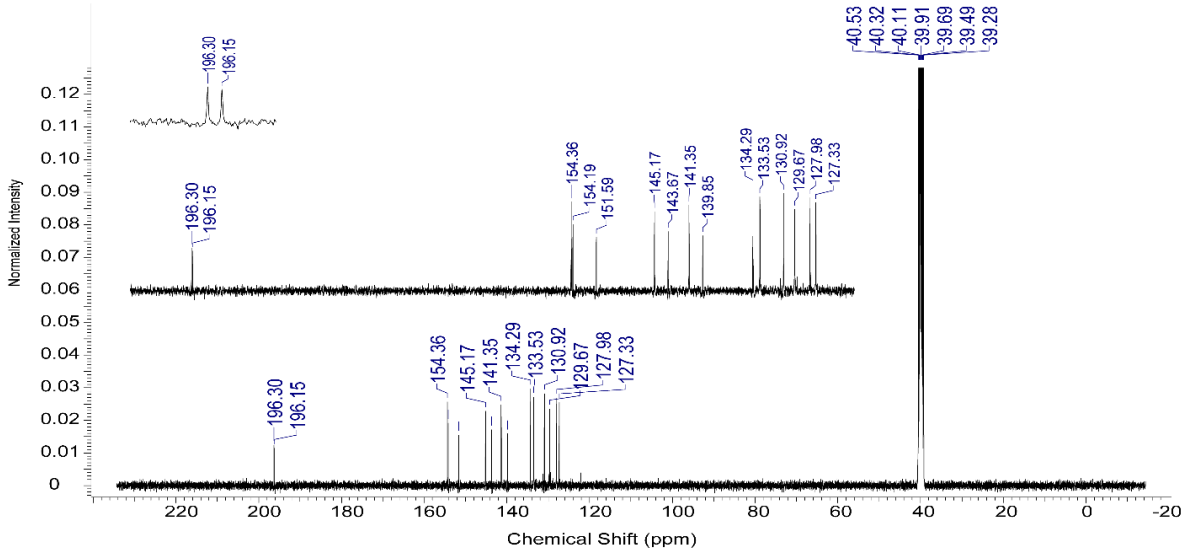

Fig. S3 ^{13}C NMR spectrum of **2** in DMSO-d_6.

Table S1 Single-crystal X-ray diffraction data of **2**.

Data	**2**
Empirical formula	$C_{15}H_9Cl_2N_3O_2Ru$
Formula weight (g·mol^{-1})	435.22
Temperature (K)	100(2)
Radiation, *l* (Å)	Mo_{Ka}, 0.71073
Crystal system	monoclinic
Space group	$P2_1/c$
Unit cell dimensions	
a (Å)	15.0410(4)
b (Å)	11.2450(3)
c (Å)	9.1142(3)
a (°)	90
b (°)	102.950(3)
g (°)	90
Volume (Å^3)	1502.34(8)
Z	4
Calculated density (Mg·m^{-3})	1.924
Absorption coefficient (mm^{-1})	1.411
F(000)	856
Theta range for collection	2.283 to 31.047°
Reflections collected	17386
Unique reflections	3875
Minimum/maximum transmission	0.579/1.000
Refinement method	Full-matrix least-squares on F^2
Data / parameters / restraints	3875 / 208 / 0
Goodness-of-fit on F^2	1.090
Final *R* indices [$I>2s(I)$]	R_1 = 0.0382, wR_2 = 0.1041
R indices (all data)	R_1 = 0.0421, wR_2 = 0.1067
Maximum/minimum residual electron density (e·Å^{-3})	1.114 / –0.831

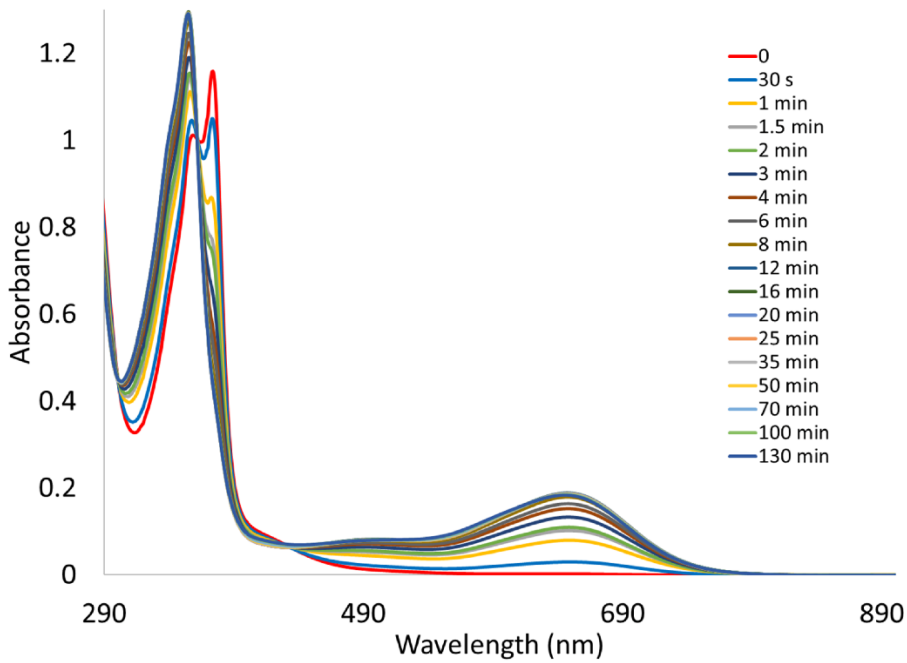

a)

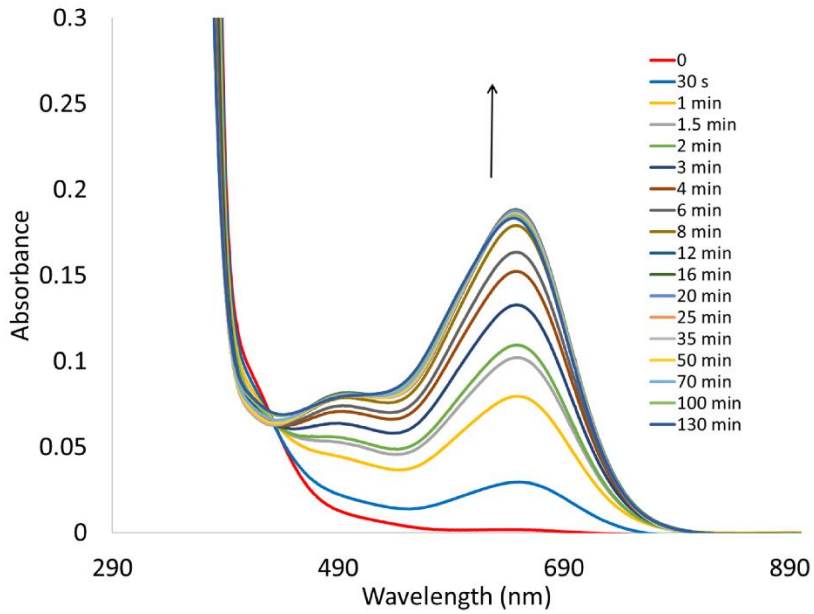

b)

Fig. S4 UV/Vis changes of **2** in DMSO upon photolysis at 468 nm with increasing illumination time (0–130 min); **a)** complete spectrum and **b)** Selected range.

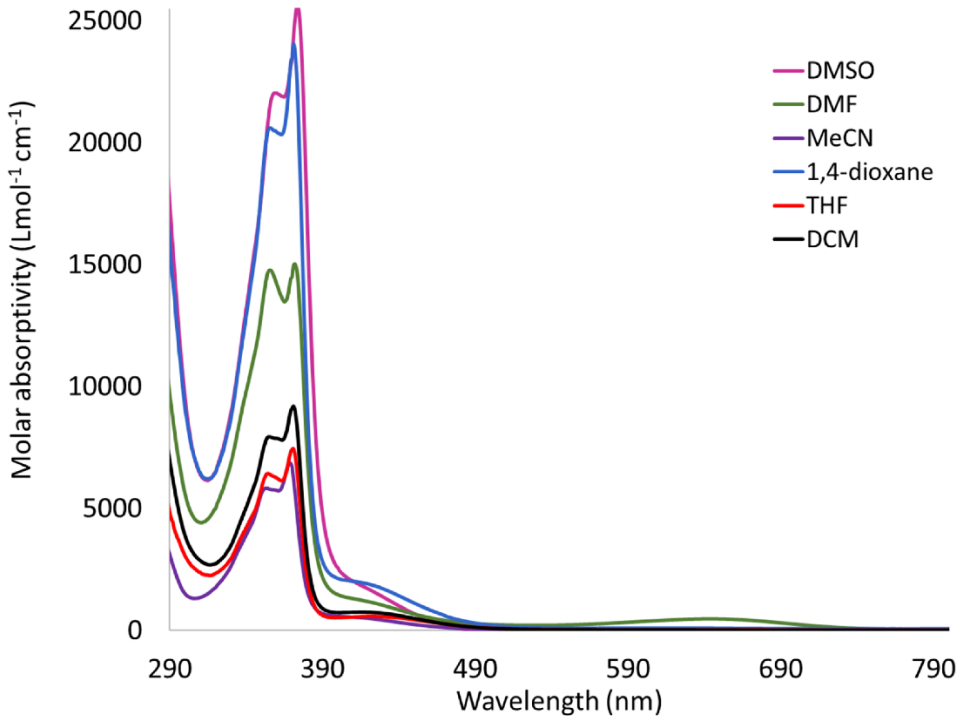

Fig. S5 The solvatochromism of **2** in different solvents.

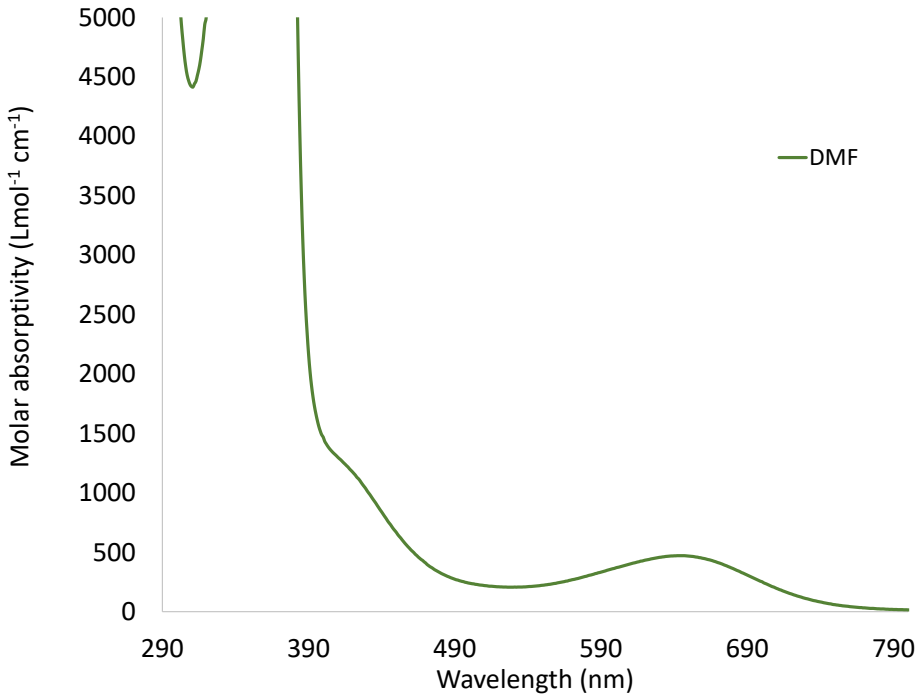

Fig. S6 Electronic absorption spectrum of **2** in DMF.

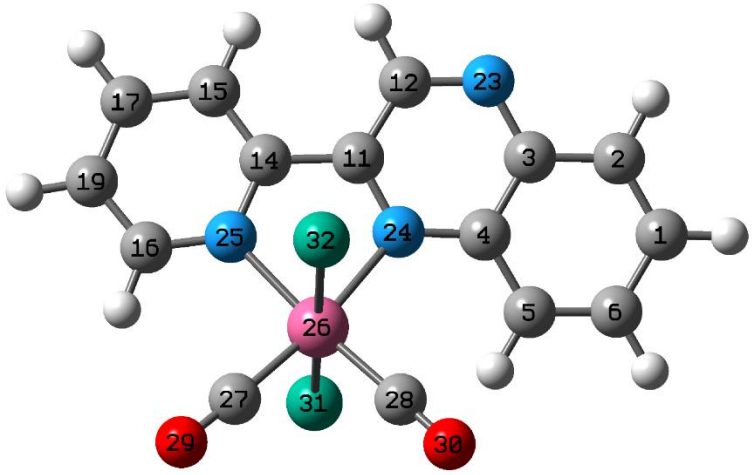

Fig. S7 The local minimum structure of 2 obtained at B3LYP/LANL2DZ level of theory (Grey balls for C, blue for N, red for O and green for Cl).

Table S2 Atomic coordinates of the optimized structure of **2**.

Center number*	Atomic number	Atomic type	Coordinates (Å)		
			X	Y	Z
1	6	0	5.052022	-0.02744	-0.2527
2	6	0	4.54011	1.217477	0.087923
3	6	0	3.132281	1.423473	0.109744
4	6	0	2.23887	0.323739	-0.17229
5	6	0	2.790776	-0.92826	-0.56173
6	6	0	4.169158	-1.09468	-0.60037
7	1	0	6.125802	-0.19027	-0.27724
8	1	0	5.177374	2.062641	0.327381
9	1	0	2.130183	-1.71948	-0.88951
10	1	0	4.581784	-2.04991	-0.91265
11	6	0	0.416431	1.791558	0.074346
12	6	0	1.331203	2.863225	0.329182
13	1	0	0.967486	3.867269	0.515492
14	6	0	-1.03569	2.001445	-0.07178
15	6	0	-1.64319	3.270158	-0.10288
16	6	0	-3.09697	0.961054	-0.54076
17	6	0	-3.02004	3.369857	-0.35626
18	1	0	-1.0568	4.167192	0.055861
19	6	0	-3.75779	2.197409	-0.59201
20	1	0	-3.63048	0.036205	-0.71847
21	1	0	-3.50279	4.342192	-0.37952
22	1	0	-4.81997	2.228971	-0.80895
23	7	0	2.64747	2.685967	0.386155
24	7	0	0.86918	0.529807	-0.0967
25	7	0	-1.77345	0.864535	-0.27138
26	44	0	-0.70825	-0.93982	0.070856
27	6	0	-2.25699	-2.01277	0.23113
28	6	0	0.316475	-2.47805	0.527036
29	8	0	-3.2408	-2.64924	0.316241
30	8	0	0.907397	-3.43881	0.85253
31	17	0	-0.58289	-1.36373	-2.37291
32	17	0	-0.79387	-0.31391	2.481246

* The atoms are numbered according to the structure depicted in **Fig. S5**.

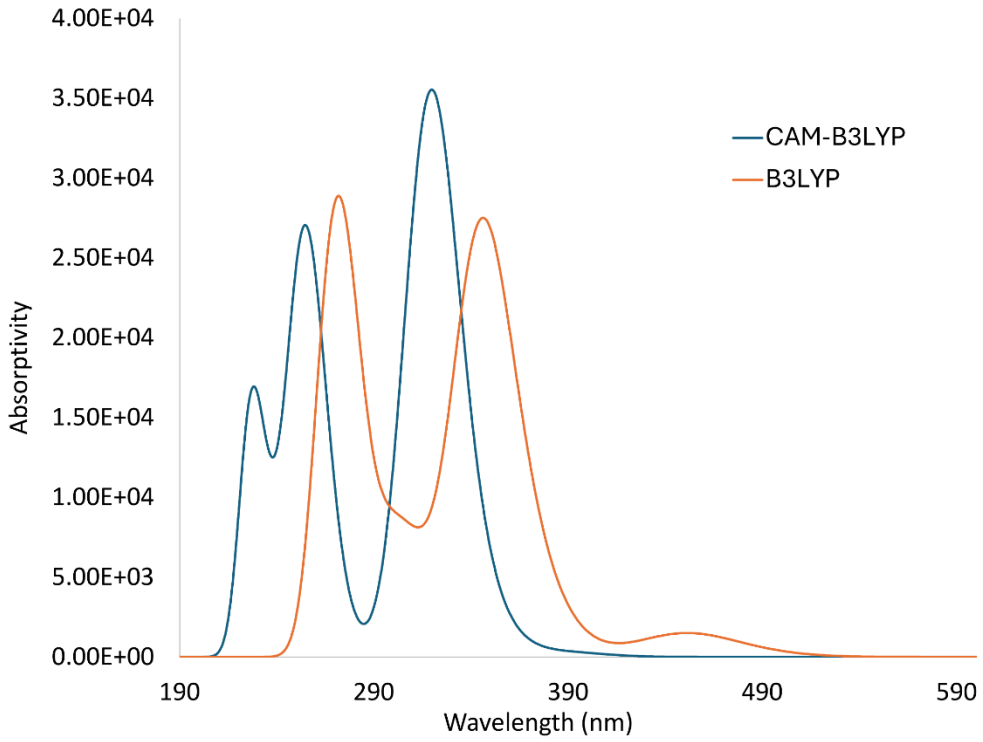

Fig. S8 Computed electronic absorption spectra of **2** at B3LYP/LANL2DZ and CAM-B3LYP/LANL2DZ level of theories.

Table S3 Computed excitation energies (eV), electronic transition configurations and oscillator strengths (*f*) of **2** at B3LYP/LANL2DZ and CAM-B3LYP/LANL2DZ level of theories (selected, *f* > 0.001) (Selected)			
Energy (cm^{-1})	Wavelength (nm)	*f*	Major contributions
✓ **B3LYP/LANL2DZ**			
21181	472	0.001	HOMO→LUMO (99%)
22189	450	0.0198	HOMO−1→LUMO (98%)
27078	369	0.0451	HOMO−2→LUMO (86%)
28594	349	0.0313	HOMO−5→LUMO (76%)
32530	307	0.0351	HOMO−7→LUMO (85%)
33392	299	0.049	HOMO→LUMO+3 (49%), HOMO→LUMO+5 (23%)
35964	278	0.0587	HOMO−2→LUMO+1 (47%)
✓ **CAM-B3LYP/LANL2DZ**			
24734	404	0	HOMO→LUMO+2 (69%)
25785	387	0.004	HOMO−1→LUMO+2 (74%)
29792	335	0.044	HOMO−1→LUMO (90%)
31253	319	0.2453	HOMO−7→LUMO (26%), HOMO-3→LUMO (30%), HOMO−2→LUMO (20%)
32310	309	0.0953	HOMO−3→LUMO (60%)
39660	252	0.1829	HOMO−6→LUMO (27%),
44215	226	0.1521	HOMO→LUMO+1 (24%)

Table S4 Selected Frontier molecular orbitals and their energies.

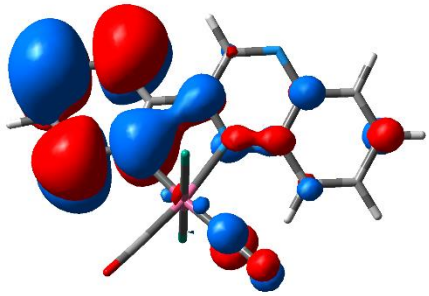 LUMO+2 (−2.23 eV)	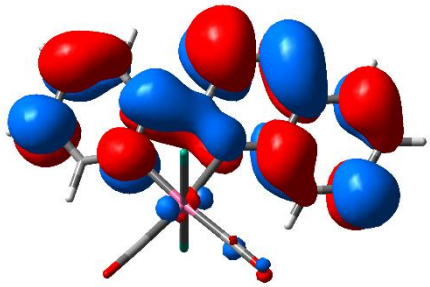 LUMO+1 (−2.45 eV)
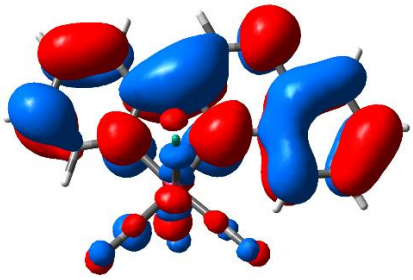 LUMO (−3.60 eV)	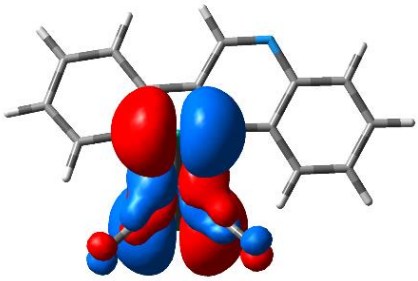 HOMO (−6.26 eV)
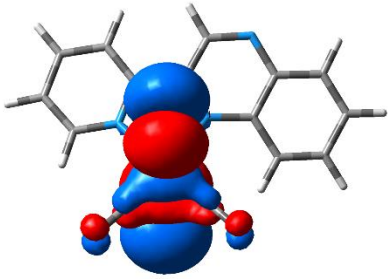 HOMO−1 (−6.32 eV)	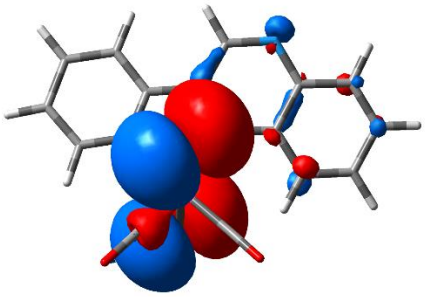 HOMO−2 (−7.01 eV)
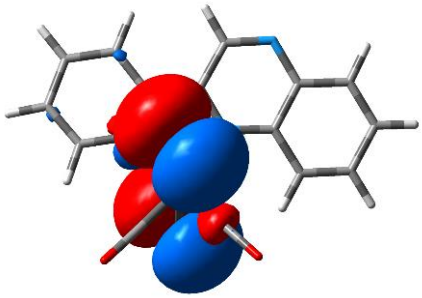 HOMO−3 (−7.04 eV)	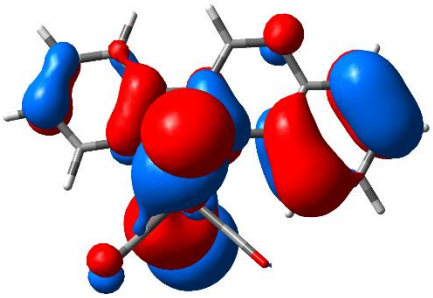 HOMO−5 (−7.62 eV)

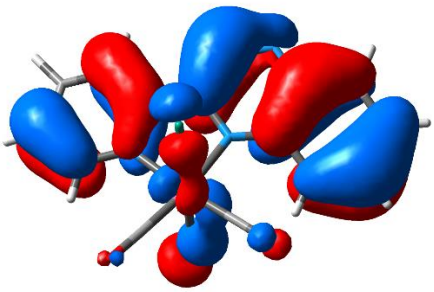 HOMO−6 (−7.87 eV)	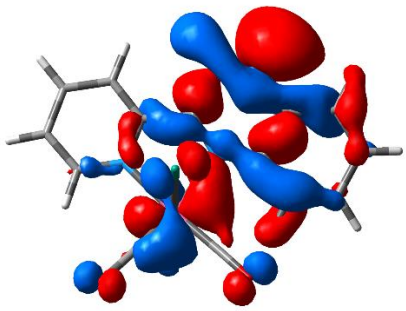 HOMO−7 (−8.05 eV)

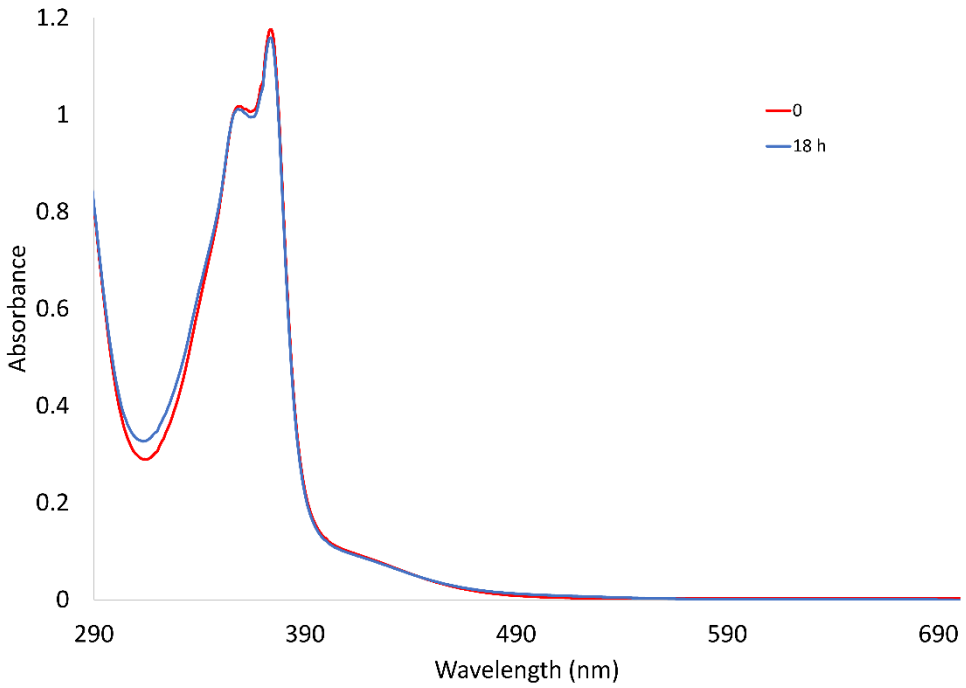

Fig. S9 The UV/Vis spectral alterations upon incubation of **2** in DMSO for 18 h.

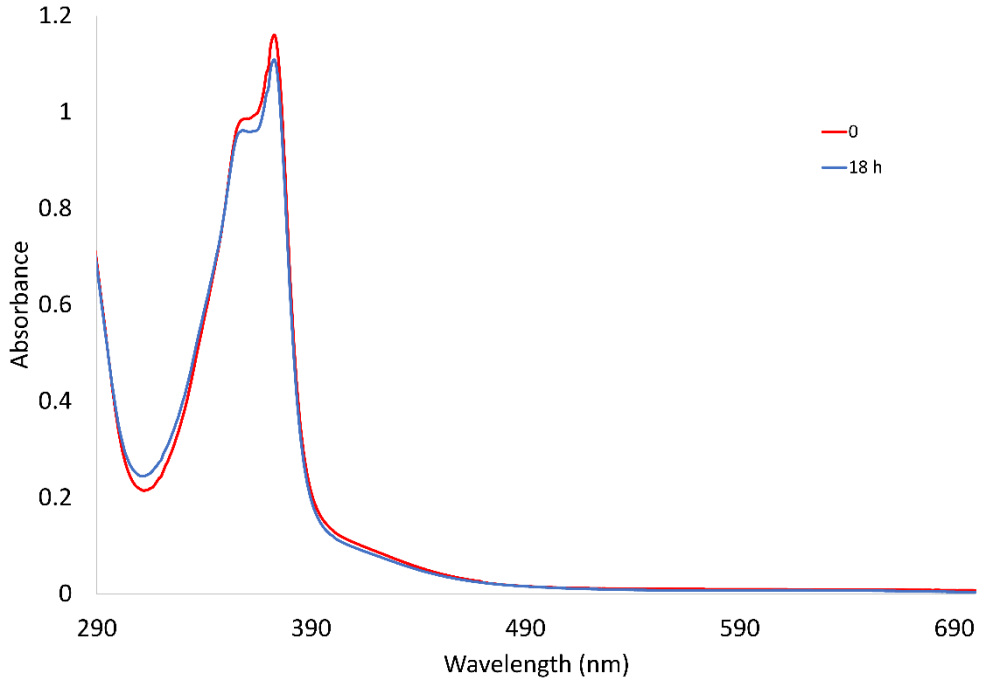

Fig. S10 The UV/Vis spectral alterations upon incubation of **2** in 70% DMSO/H_2O for 18 h.

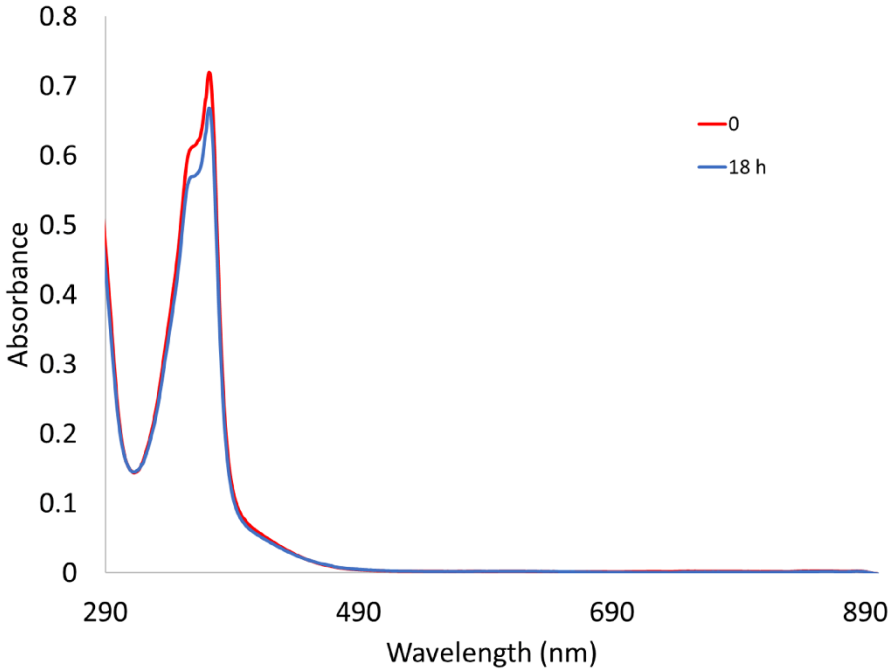
0.8
0.7
0.6
0.5
0.4
0.3
0.2
0.1
0
Absorbance
290
490
690
890
Wavelength (nm)
0
18 h

a)

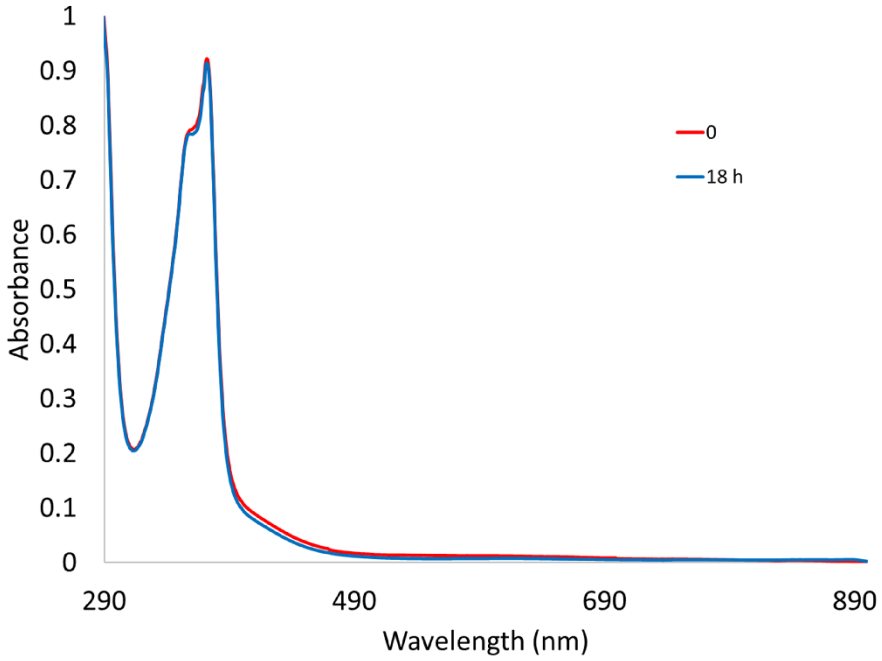
1
0.9
0.8
0.7
0.6
0.5
0.4
0.3
0.2
0.1
0
Absorbance
290
490
690
890
Wavelength (nm)
0
18 h

b)

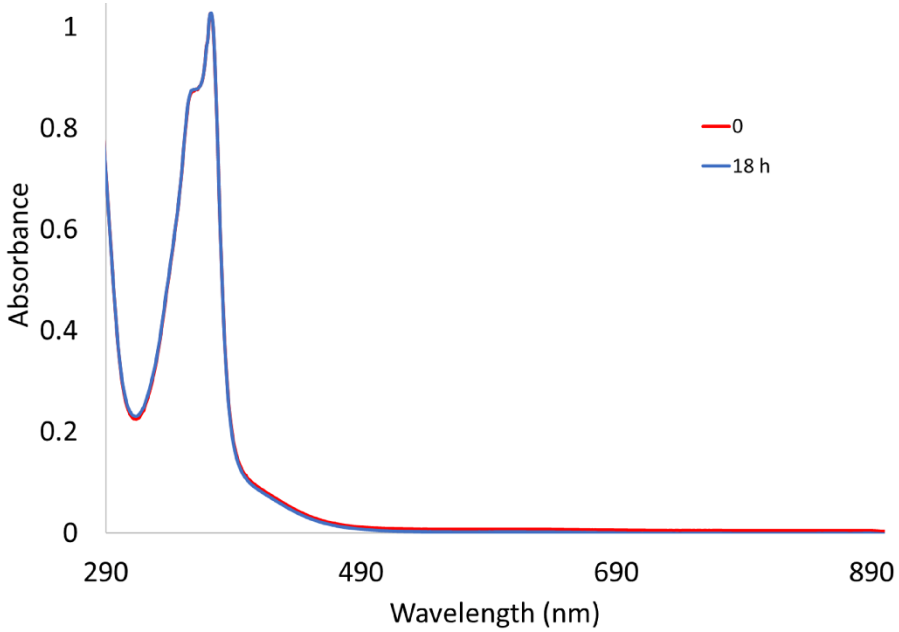

c)

Fig. S11 The UV/Vis spectral alterations upon incubation of **2** in 70% aqueous DMSO for 18 h in presence of **a)** histidine, **b)** HEWL and **c)** CT-DNA.

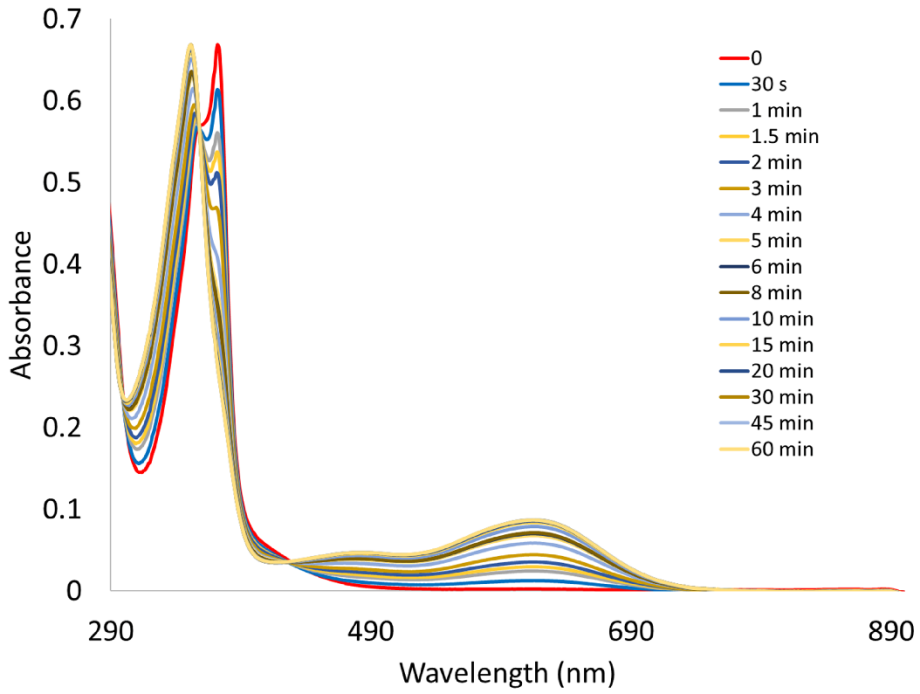

a)

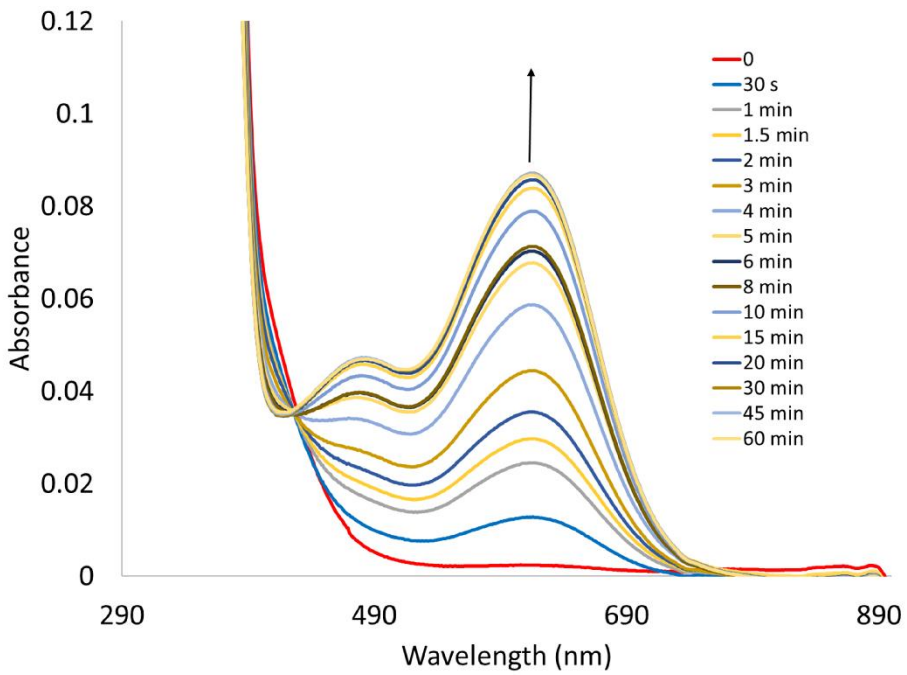

b)

Fig. S12 UV/Vis changes of **2** in 70% DMSO/H_2O in presence of histidine upon photolysis at 468 nm with increasing illumination time (0–60 min); **a)** complete spectrum and **b)** Selected range.

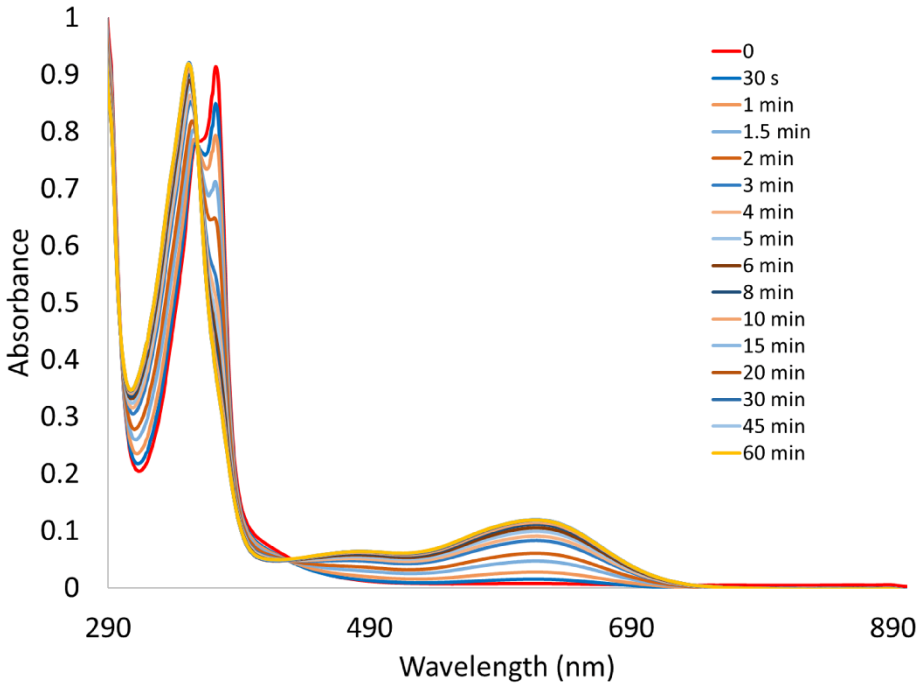

a)

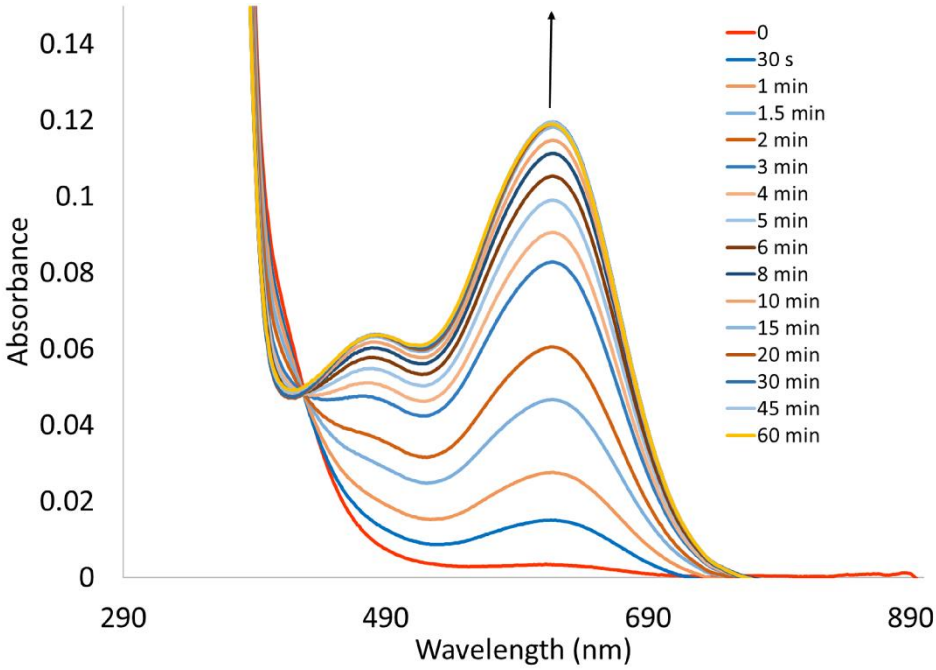

b)

Fig. S13 UV/Vis changes of **2** in 70% DMSO/H_2O in presence of HEWL upon photolysis at 468 nm with increasing illumination time (0–60 min); **a)** complete spectrum and **b)** Selected range.

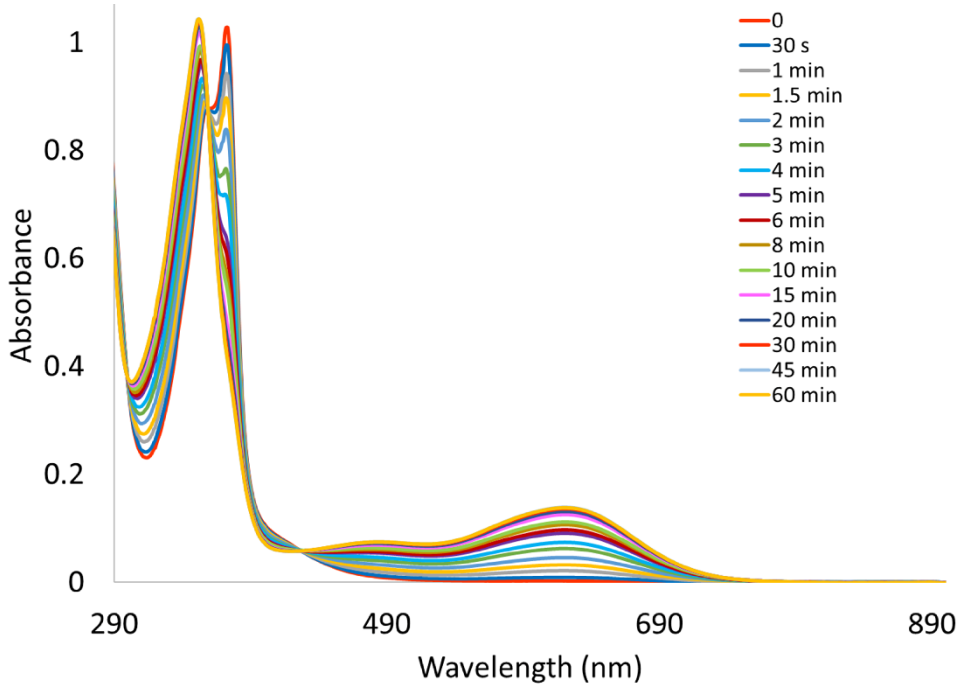

a)

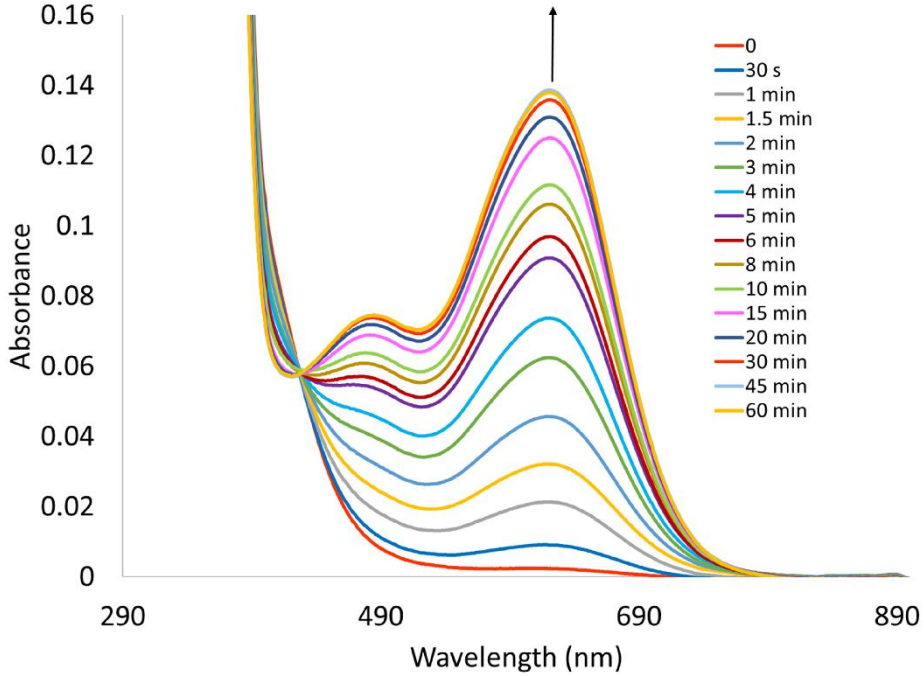

b)

Fig. S14 UV/Vis changes of **2** in 70% DMSO/H_2O in presence of CT-DNA upon photolysis at 468 nm with increasing illumination time (0–60 min); **a)** complete spectrum and **b)** Selected range.

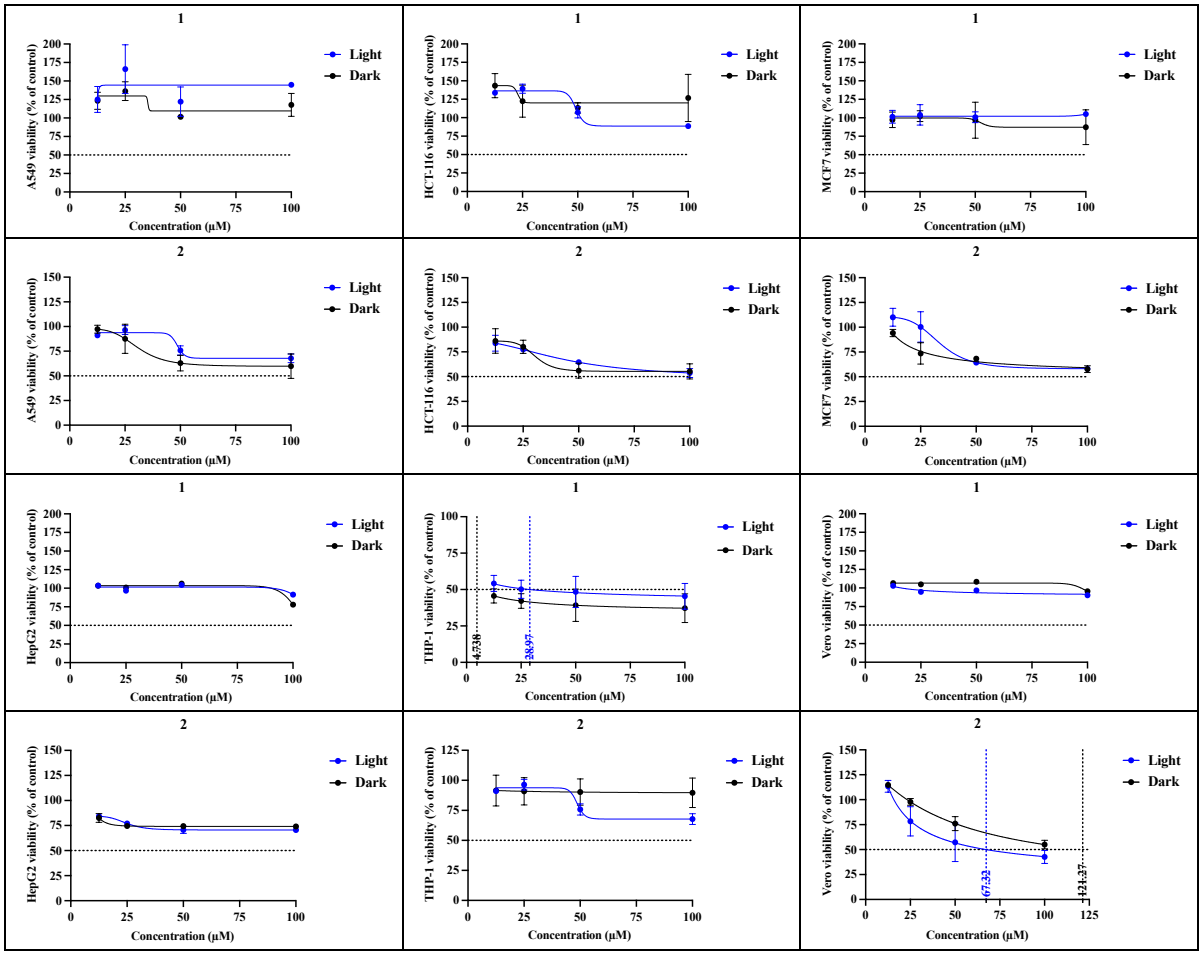

Fig. S15 The dose-response curves of **1** and **2** against MCF7, HepG2, A549, HCT-116, THP-1, and normal Vero cell line, at dark and light conditions using the MTT assay.

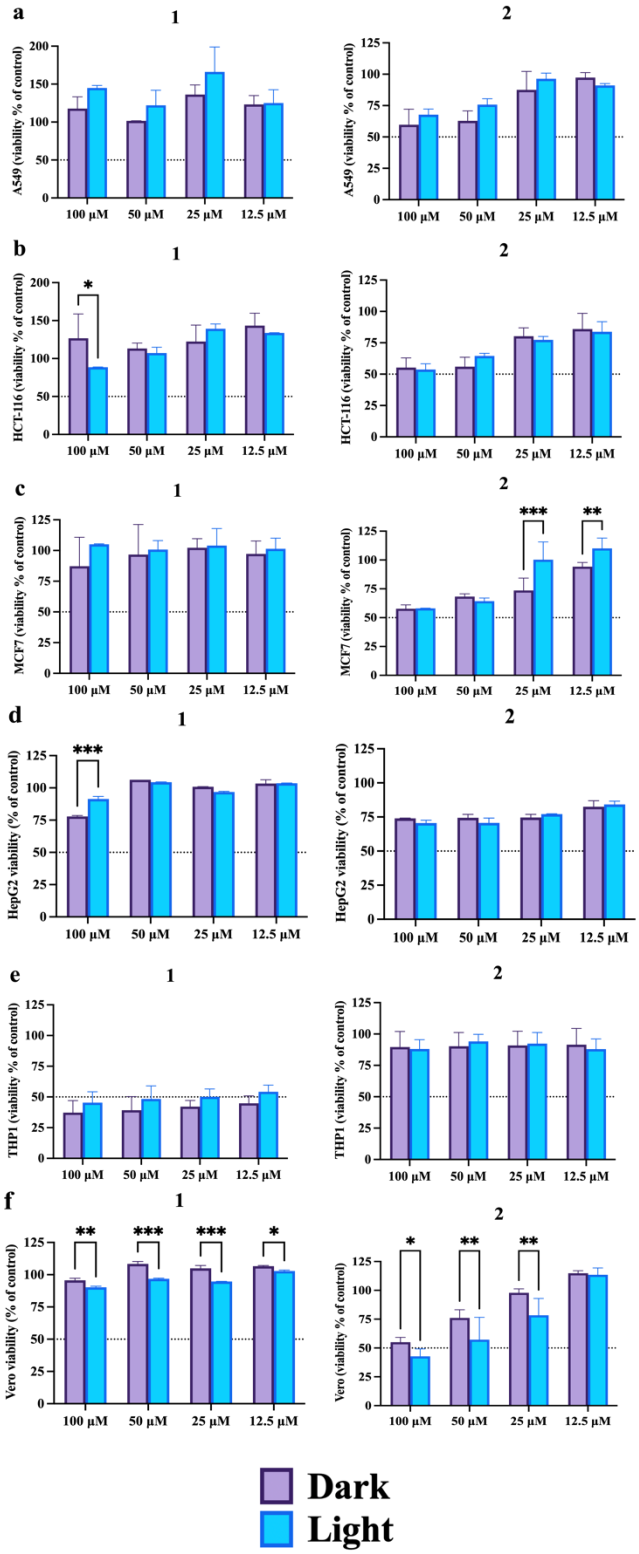

Fig. S16 The cell viability of **1** and **2** in dark and light conditions on **a)** A549, **b)** HCT-116, **c)** MCF7, **d)** HepG2, **e)** THP-1, and f) Vero cell line. Using 2-way ANOVA with Šídák's multiple comparisons tests were performed at a 95% confidence interval to detect significant differences between dark and light conditions at various concentrations. * $p < 0.05$, ** $p < 0.01$, *** $p < 0.001$. The data are represented as mean ± SD.